

Preparation and characterization of nanocrystalline transition metal-loaded sulfated titania through sol–gel method

K.R. Sunajadevi, S. Sugunan*

Department of Applied Chemistry, Cochin University of Science and Technology, Kochi-682 022, India

Received 25 December 2003; accepted 3 June 2004

Available online 23 July 2004

Abstract

Transition metal-loaded (3%) nanocrystalline sulfated titania (ST) powders are prepared using the sol–gel technique. Anatase is found as the active phase in all the samples. Sulfate ion impregnation decreases the crystallite size and stabilizes the anatase phase of TiO₂. Acidity of the samples is found to increase by the incorporation of sulfate ion and also by the modification by transition metal ions. All the prepared catalysts are found stable up to 700 °C.

© 2004 Published by Elsevier B.V.

Keywords: Sol–gel processing; Nano materials; Titania; Sulfated titania

1. Introduction

In recent years, research work in the area of particles of small size (1–10 nm) has received much attention. There have been quite intense works in the methodology of preparation and stabilization of these particles and studying their physical and chemical properties. Sol–gel method represents a useful route in the synthesis of supported metal catalysts. Advantages of the method includes

- (i) superior homogeneity and purity
- (ii) better microstructural control of the support
- (iii) higher BET surface areas
- (iv) well-defined pore size distributions
- (v) improved thermal stability of the supported metal particles and
- (vi) ease with which the additional elements may be added.

Sol–gel method have attracted much interest in the preparation of titania powders and colloids because of

the many uses of this material, as a pigment, filler and more recently, as a membrane, antireflection coating, catalyst and photocatalyst. Titania sol–gel synthesis has been developed from inorganic precursors and from metal organic Ti(OR)₄ precursors [1]. When titania is prepared by sol–gel method, it can be obtained with a crystallite size in the range of nanometers. Titanium dioxide is known to exist in three crystalline modifications, namely rutile (tetragonal), anatase (tetragonal) and brookite (orthorhombic). Anatase and rutile are the common polymorphs of synthetic titania. In fact, crystallization is highly influenced by the hydrolysis condition [2]. During the condensation process, the formation of the kinked chains of edge-sharing octahedra corresponding to anatase appears more probable than the formation of straight chains typical of rutile. Therefore, anatase is obtained in processes under kinetic control, whereas processes involving Ostwald riping lead to the equilibrium phase, i.e., rutile [3]. On the other hand, the brookite structure, in which each octahedron shares one edge, has not been X-ray-characterized to date, to our knowledge, in sol–gel process.

The chemical and catalytic properties of titania can be modified by the incorporation of metallic ions. Some metal oxides, when sulfated, develop the ability to

* Corresponding author. Tel.: +91 484 2575804; fax: +91 484 2577595.

E-mail address: ssg@cusat.ac.in (S. Sugunan).

catalyze reactions characteristic of very strong acid catalysts at low temperatures, although with limited life times. In recent years, considerable research attention has been directed towards a number of sulfated metal oxide systems [4–6]. In such systems, it has been demonstrated that the way in which materials are prepared is of crucial importance. The temperature of calcination to produce the most active materials is dependent upon the identity of the oxide and sulfation reagent. In this communication, we are reporting the effect of metal incorporation on nanocrystalline sulfated titania (ST) and their physicochemical characterization.

2. Experiments

2.1. Sample preparation

Cr, Mn, Fe, Co, Ni, Cu and Zn-loaded (3%) sulfated titania nano powders were prepared by sol–gel process which was shown in Fig. 1. Titanium isopropoxide (98%, Aldrich) was used as the precursor of titania. An amount, 25 ml, of $\text{Ti}(\text{OC}_3\text{H}_7)_4$ was hydrolyzed in 300 ml water containing 2.5 ml nitric acid. Precipitates formed were stirred continuously at room temperature to form a highly dispersed sol. To this, Cr, Mn, Fe, Co, Ni, Cu and Zn nitrate solutions (3 wt.%) were added separately and stirred again for about 4 h. After keeping the sol for aging, it was concentrated and dried at 60°C . Sulfation was done using 0.5 M sulfuric acid solution (2 mL g^{-1} of the hydroxide). The samples, after overnight drying at 110°C , were calcined for 5 h at 500°C . The general sample notation STX3 stands for sulfated titania with 3 wt.% of X metal

oxide, whereas T and ST denotes pure and sulfated titania, respectively.

2.2. Sample characterization

X-ray powder diffraction (XRD) patterns have been recorded on a Rigaku D-max C X-ray diffractometer using Ni-filtered $\text{Cu K}\alpha$ radiation source ($\lambda=0.15406\text{ nm}$). Micromeritics Gemini-2360 surface area analyzer was used to determine the BET surface area under liquid nitrogen temperature, using nitrogen gas as the adsorbent. Previously activated samples at 500°C were degassed at 400°C under nitrogen atmosphere for 4 h prior to each measurement. The pore volumes of the samples were also measured using the same instrument by the uptake of nitrogen at a relative pressure of 0.9. Thermal analysis between room temperature and 800°C were carried out in N_2 atmosphere, with a ramp of $20^\circ\text{C min}^{-1}$ using a TGAQ V2.34 thermal analyzer (TA instruments make). FTIR spectra were recorded on a Magna 550 Nicolet instrument in the range of $4000\text{--}400\text{ cm}^{-1}$ on KBr phase. Element of the samples was analyzed by EDX measurements using EDX-JEM-35 instrument (JEOL link system AN-1000 Si–Li detector). Diffuse reflectance UV-VIS spectra of the samples were recorded at room temperature between 200 and 800 nm, using MgO as standard in the Ocean Optics AD 2000 instrument with CC detector. To determine the acidity of the catalysts, ammonia TPD measurements in the range of $100\text{--}600^\circ\text{C}$ were performed in a conventional flow-type apparatus at a heating rate of $20^\circ\text{C min}^{-1}$ and in a nitrogen atmosphere [7]. The acidity determination was supported by the TGA studies using 2,6-dimethylpyridine (DMP) as a probe molecule. Pre-

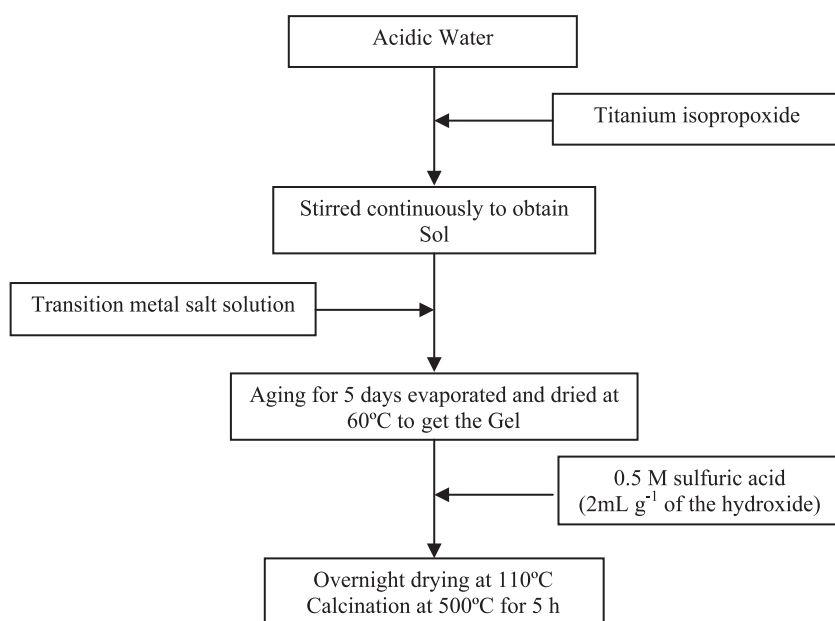


Fig. 1. Preparation process of transition metal loaded sulfated titania powders.

Table 1
Textural parameters of the prepared systems

Catalyst	BET surface area ($\text{m}^2 \text{g}^{-1}$)	Pore volume ($\times 10^{-6} \text{m}^3 \text{g}^{-1}$)	Crystallite size (nm)	Pore diameter (nm)	Elemental composition from EDX (%)		
					TiO ₂	SO ₄	Metal
T	35	0.09	12.71	102.8	100	–	–
ST	91	0.21	9.62	92.3	95.34	4.66	–
STCr3	100	0.18	5.90	72.0	88.05	9.16	2.78
STMn3	87	0.15	7.09	69.0	90.49	7.28	2.23
STFe3	104	0.17	10.40	65.4	89.44	7.83	2.98
STCo3	90	0.14	7.89	62.2	89.81	7.83	2.36
STNi3	83	0.15	12.62	72.3	89.43	8.34	2.23
STCu3	70	0.15	9.02	85.7	89.89	7.47	2.67
STZn3	92	0.14	9.83	60.1	89.11	8.14	2.75

viously activated catalysts were kept in a desiccator saturated with vapours of 2,6-DMP at room temperature for 48 h and then subjected to thermal analysis in N₂ atmosphere at a heating rate of 20°C min⁻¹. Their fraction of weight loss in the range of 300–600°C was found out and was taken as a measure of Brönsted acidity of the samples.

3. Results and discussion

3.1. XRD and EDX analysis

All peaks measured by XRD analysis could be assigned to those of TiO₂ crystal. The average crystallite size is calculated (Table 1) using Scherrer [8] equation from the

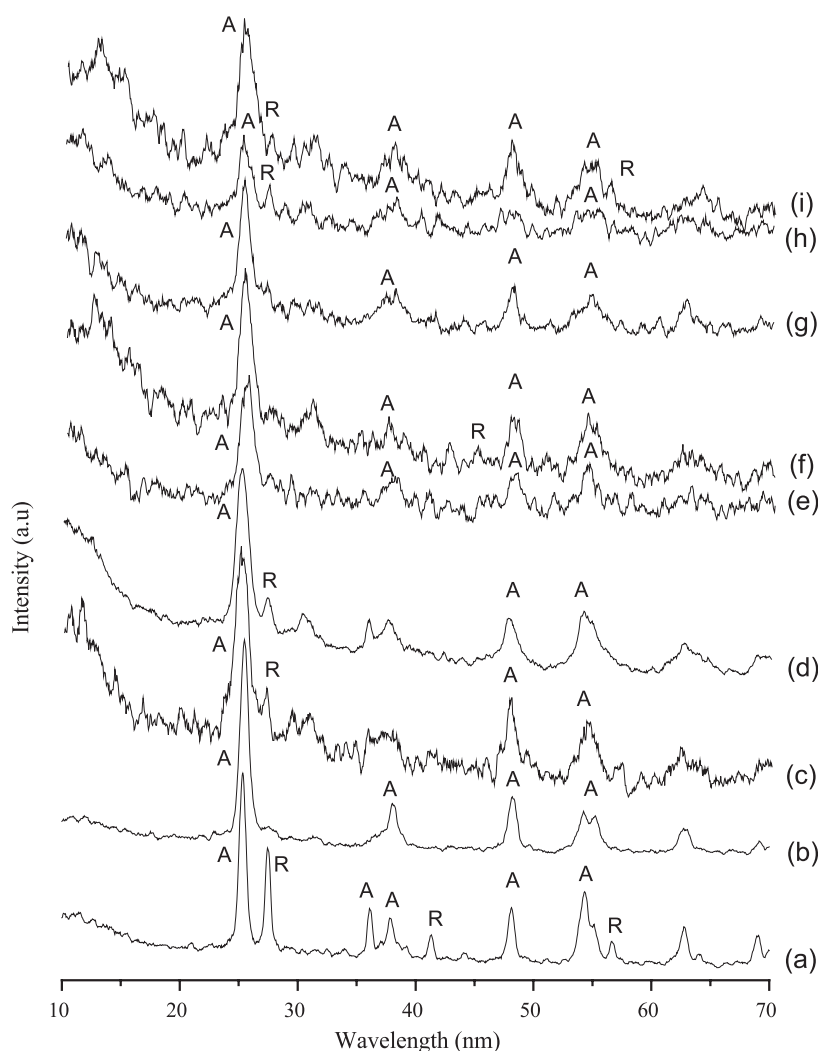


Fig. 2. XRD profiles of T (a), ST (b), STCr3 (c), STMn3 (d), STFe3 (e), STCo3 (f), STNi3 (g), STCu3 (h) and STZn3 (i). A, anatase; R, rutile.

(101) reflection of anatase. Fig. 2 shows the XRD profiles of the samples calcined at 500°C. Pure titania shows two main peaks at $2\theta=25.4^\circ$ and 27.5° , corresponding to (101) phase of anatase and (110) phase of rutile, respectively. In the case of sulfated titania (ST), there is no peak corresponding to rutile, which means sulfation retards the transformation from anatase to rutile. No peaks corresponding to the transition metal oxide is detected, suggesting that it exist as the amorphous phase without getting incorporated into the TiO_2 phase; that is, they are in a highly dispersed form on the surface. The crystallite size calculated using Scherrer equation reveals that all the samples are in nanometer range. Incorporation of metal ions again decreases the crystallite size. The EDX data (Table 1) shows the surface composition of the sulfated systems. The sulfate content of the metal incorporated samples is considerably higher, when compared with simple sulfated system, which indicates that metal doping brings about a considerable reduction in the extent of sulfate loss from the catalyst surface. Although the same concentration of sulfuric acid solution was used for sulfate modification of all the samples, their sulfate-retaining

capacity is different. The fact that the presence of these metal oxides stabilizes the sulfate over layers on the catalyst surface is thus apparent from the increase in the sulfate-retaining capacity. The absence of any change in the peak intensity in XRD after sulfate treatment indicates that the amount of sulfate retained on the surface is insufficient to cause any change in the diffraction pattern and that it is well dispersed on the surface without entering into the bulk of the catalyst.

3.2. BET surface area, pore volume measurements and thermal analysis

The sulfated samples showed a higher surface area compared to pure titania (Table 1). Sulfation reduces the extent of surface area loss during high-temperature calcinations. This can be explained based on higher resistance to sintering as well as the delayed transformation from amorphous to crystalline state acquired by doping with sulfate ions [9,10]. For the metal incorporated systems, there is not much difference in the surface area and pore volume. The small difference is due

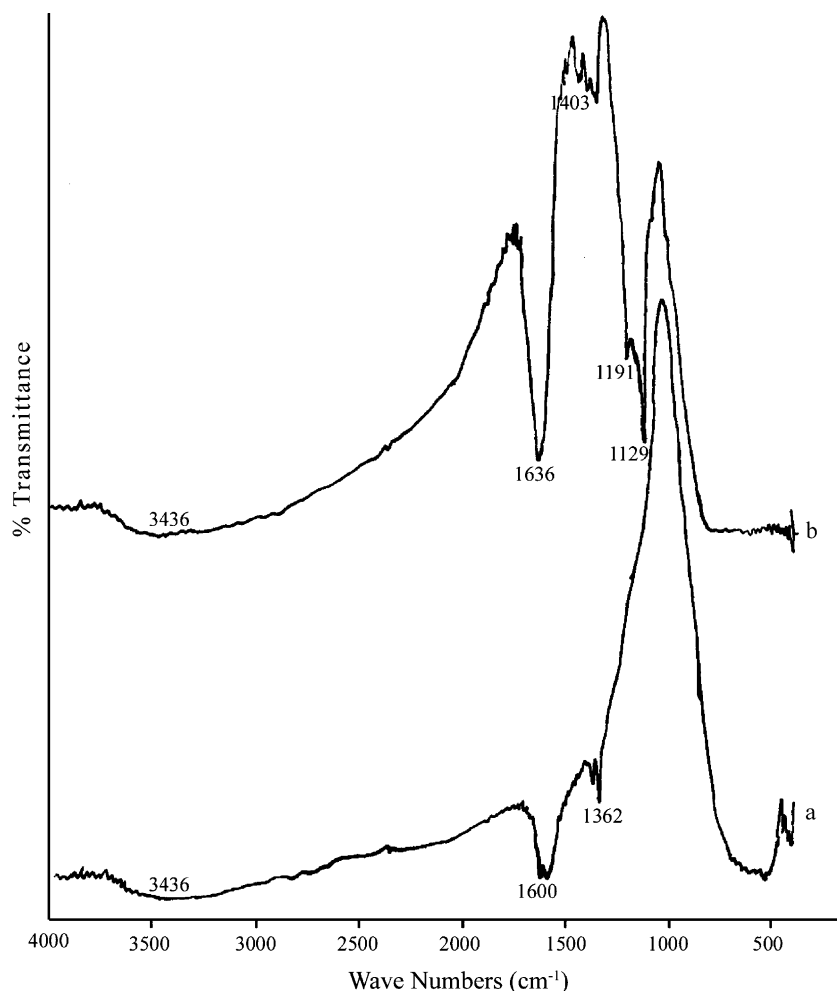


Fig. 3. FTIR spectra of T (a) and ST (b).

to the difference in the sulfate content of the systems. The preferential attachment of these sulfate groups at the edges of pores leading to the partial filling of the pores, which reduces the effective radii and leads to small changes in the surface area and pore volume. The addition of transition metal resulted in a slight lowering of the crystallite size, which may be a consequence of the fine dispersion of the sulfate and metal species on the surface. This also results in the higher surface area of the catalyst. Addition of transition metal species causes a further

setback to the crystallization and sintering process, which is evident from the higher surface area of the samples in comparison with the simple sulfated system. The metal oxide species, along with the sulfate ions, prevent the agglomeration of titania particles, resulting in a higher surface area. Thermal analysis of the samples shows mainly two weight loss regions, one corresponding to loss of physisorbed water below 150 °C, the second one revealing the commencement of decomposition of sulfate into SO_2/SO_3 vapours above 700 °C. The metal-incorpo-

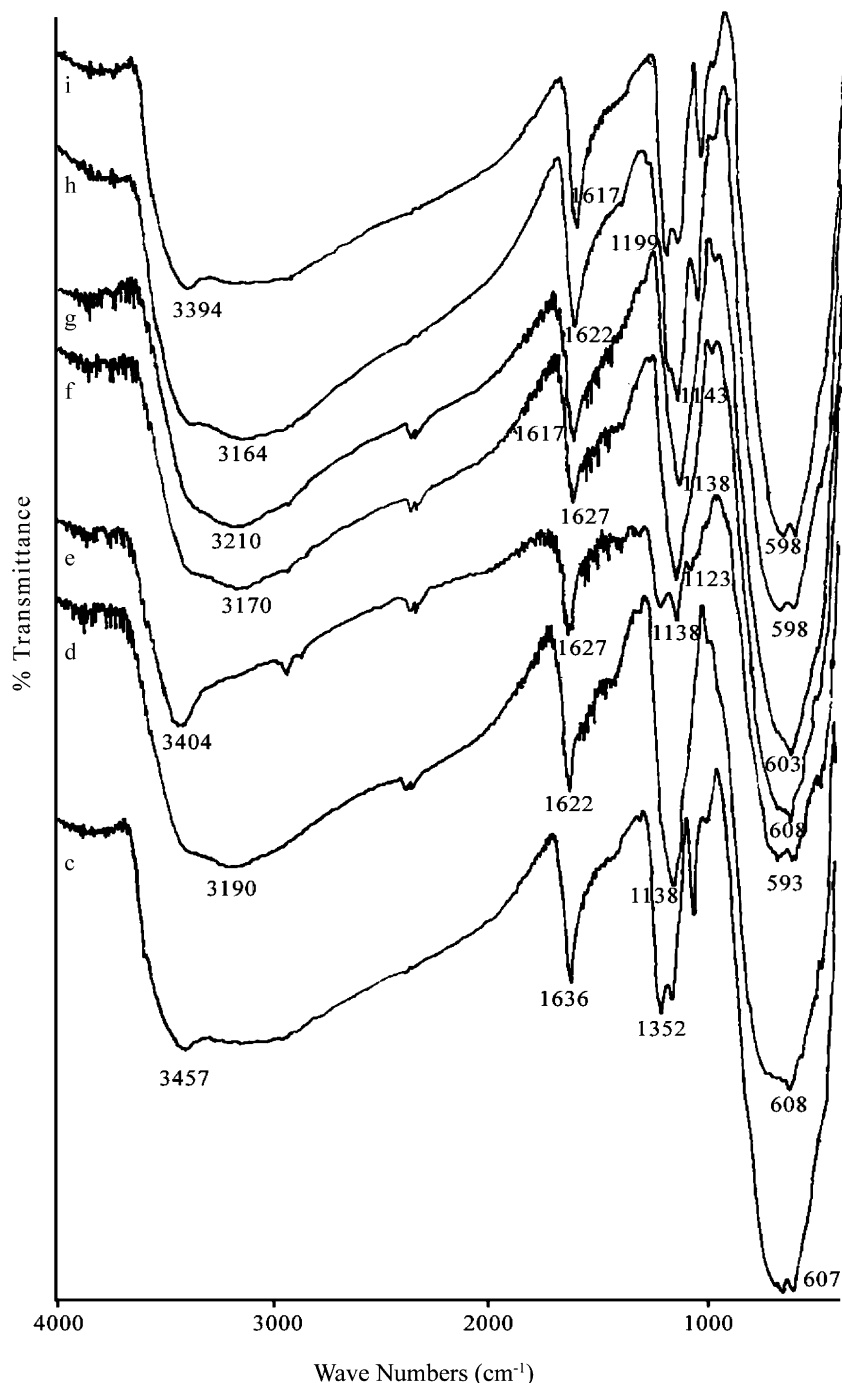


Fig. 4. STCr3 (c), STMn3 (d), STFe3 (e), STCo3 (f), STNi3 (g), STCu3 (h) and STZn3 (i).

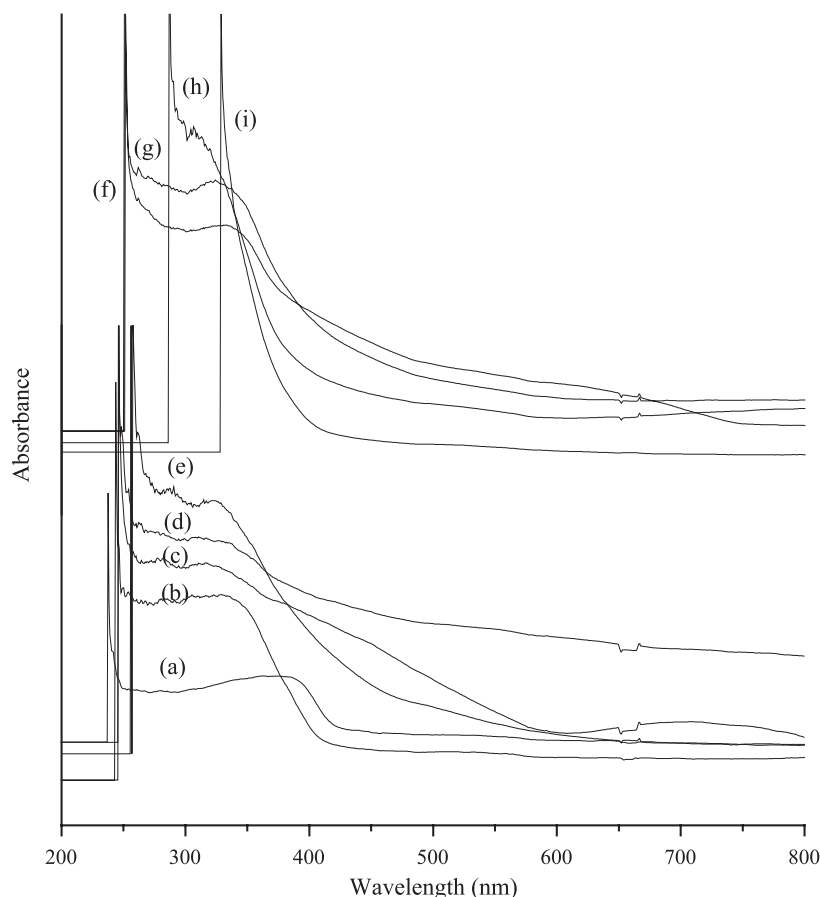


Fig. 5. UV-VIS DR spectra of T (a), ST (b), STCr3 (c), STMn3 (d), STFe3 (e), STCo3 (f), STNi3 (g), STCu3 (h) and STZn3 (i).

rated samples exhibited a higher thermal stability. It is inferred that besides delaying the crystallization process, the addition of the metal species also serves to stabilize the surface sulfate species.

3.3. FTIR and UV-VIS DR spectral analysis

FTIR spectra (Figs. 3 and 4) of the sulfated systems shows a peak at $1200\text{--}1100\text{ cm}^{-1}$ which can be assigned to S=O group [11]. The peak around 1400 cm^{-1} suggests that the added sulfate exists as SO_4^{2-} species. The bands around 1636 and 3436 cm^{-1} correspond to the bending

and stretching modes of the –OH groups present in the catalysts. The IR spectra of the modified samples do not show any band corresponding to the transition metal oxide, which confirms the XRD result. UV-VIS diffuse reflectance spectroscopy (Fig. 5) permits the detection of framework Ti in the samples. In all the samples, characteristic band for tetrahedrally coordinated titanium appears at about $300\text{--}380\text{ nm}$. A progressive red shift in the band-gap absorption is noticed with metal loading. The absorption is associated to the $\text{O}^{2-} \rightarrow \text{Ti}^{4+}$ charge-transfer, corresponding to electronic excitation from the valence band to the conduction band.

Table 2
Surface acidity obtained from ammonia TPD and 2,6-DMP desorption

Catalyst	Amount of ammonia desorbed (mmol g^{-1})				Weight loss (%) of 2,6-DMP desorbed
	Weak ($100\text{--}200\text{ }^\circ\text{C}$)	Medium ($200\text{--}400\text{ }^\circ\text{C}$)	Strong ($400\text{--}600\text{ }^\circ\text{C}$)	Total ($100\text{--}600\text{ }^\circ\text{C}$)	
T	0.3108	0.2019	0.0103	0.5230	0.77
ST	0.5010	0.3221	0.0895	0.9126	5.17
STCr3	0.5620	0.5924	0.2898	1.4442	5.60
STMn3	0.4988	0.4110	0.1165	1.0263	2.53
STFe3	0.4798	0.3203	0.1559	0.9460	2.31
STCo3	0.4947	0.3392	0.0921	0.9260	5.47
STNi3	0.4889	0.3908	0.0431	0.9228	5.13
STCu3	0.5039	0.3793	0.0554	0.9386	5.84
STZn3	0.4959	0.3434	0.1459	0.9852	3.43

3.4. Acidity measurements

NH₃-TPD is now widely used for evaluating the surface acidity of the solid catalysts [12,13]. The distribution of acid sites and total acidity values of the different systems are shown in Table 2. The ammonia thermodesorption results give clear evidence for the presence of surface acid sites of different strength going from weak to strong acidities. Pure titania shows only low acidity, and sulfation increases its acidity. Incorporation of metal ions considerably changes the acidity. The nature of the acid sites is greatly altered by the nature of the ions incorporated into the lattice. The distribution change may be a coupled effect of the crystalline and structural changes. The change in the acid strength distribution for the different systems may be related to the interaction of the added metal cations with the TiO₂.

The thermodesorption study of 2,6-DMP was carried out with an intention of obtaining a comparative evaluation of the Brønsted acidity in the samples. Satsuma et al. [14] reported a complete elimination of the coordinately adsorbed 2,6-DMP after purging at an appropriate temperature (above 300 °C). Thus, we presume the amount of 2,6-DMP desorbed at temperatures above 300 °C to be due to desorption from Brønsted acid sites and the results are represented in Table 2. The Brønsted acidity increases in the case of metal-loaded systems, compared to pure titania. Among the different metal-incorporated system, manganese, iron and zinc shows low Brønsted acid sites, while other metal ions do not show much changes.

4. Conclusion

Nanocrystalline materials of crystallite size up to 5 nm can be easily prepared by this sol–gel method. Anatase is found to be the major phase in all the samples. Sulfation

delays the transformation from anatase to rutile. Sulfation and metal ion incorporation increased the acidity of titania. All the systems are found to be stable up to 700 °C.

Acknowledgement

The authors are thankful to Regional Sophisticated Instrument Facility (RSIC), Indian institute of Technology (IIT) Bombay, India for FTIR analysis. K.R. Sunajadevi thanks the Council of Scientific and Industrial Research, New Delhi, India, for providing the senior research fellowship.

References

- [1] J. Livage, M. Henry, C. Sanchez, *Prog. Solid. State Chem.* 18 (1988) 259.
- [2] K. Terabe, K. Kato, H. Miyazaki, S. Yamaguchi, A. Imai, Y. Iguchi, *J. Mater. Sci.* 29 (1994) 1617.
- [3] J.P. Jolivet, *De ea solution a' l' oxyde*, InterEdition, Paris, 1994, p. 98.
- [4] T. Yamaguchi, *Appl. Catal.* 761 (1990) 1.
- [5] A. Corma, *Chem. Rev.* 95 (1995) 559.
- [6] K. Arata, *Appl. Catal. A* 146 (1996) 3.
- [7] D.K. Chakrabarty, *Adsorption Catalysis by Solids*, Wiley Eastern, 1990, New Delhi, p. 15.
- [8] H. Lipson, H. Steeple, *Interpretation of X-ray Powder Diffraction Patterns*, Macmillan, London, 1970, p. 261.
- [9] K. Arata, *Adv. Catal.* 37 (1990) 165.
- [10] T. Yamaguchi, K. Tanabe, Y.C. Kung, *Mater. Chem. Phys.* 16 (1986) 67.
- [11] O. Saur, M. Bensitel, A.B.M. Saad, J.C. Lavalley, C.P. Tripp, B.A. Morrow, *J. Catal.* 99 (1986) 104.
- [12] S. Lin, R. Hsu, *J. Chem. Soc. Chem. Commun.* (1992) 1469.
- [13] F. Arene, R. Dario, A. Parmaliana, *Appl. Catal., A Gen.* 170 (1998) 127.
- [14] A. Satsuma, Y. Kamiya, Y. Westi, T. Hattori, *Appl. Catal., A Gen.* 194–195 (2000) 253.